Multifractality in individual honeybee behavior hints at colony-specific social cascades: Reanalysis of radio-frequency identification data from five different colonies

Nicole S. Carver and Damian G. Kelty-Stephen
Department of Psychology, Grinnell College, 1116 8th Ave., Grinnell, Iowa 50112, USA
(Received 3 September 2016; revised manuscript received 18 January 2017; published 13 February 2017)

Honeybees (*Apis mellifera*) exhibit complex coordination and interaction across multiple behaviors such as swarming. This coordination among honeybees in the same colony is remarkably similar to the concept of informational cascades. The multifractal geometry of cascades suggests that multifractal measures of individual honeybee activity might carry signatures of these colony-wide coordinations. The present work reanalyzes time stamps of entrances to and exits from the hive captured by radio-frequency identification (RFID) sensors reading RFID tags on individual bees. Indeed, both multifractal spectrum width for individual bees' inter-reading interval series and differences of those widths from surrogates significantly predicted not just whether the individual bee's hive had a mesh enclosure but also predicted the specific membership of individual bees in one of five colonies. The significant effects of multifractality in matching honeybee activity to type of colony and, further, matching individual honeybees to their exact home colony suggests that multifractality quantifies key features of the colony-wide interactions across many scales. This relevance of multifractality to predicting colony type or colony membership adds additional credence to the cascade metaphor for colony organization. Perhaps, multifractality provides a new tool for exploring the relationship between individual organisms and larger, more complex social behaviors.

DOI: 10.1103/PhysRevE.95.022402

I. INTRODUCTION

Honeybees (*Apis mellifera*) typify a classic challenge posed by a variety of social biological systems [1]. Namely, their swarms and colonies exhibit a collective behavior suggesting coordination and integration across many scales of space and time despite the relative autonomy, individual specialization and role switching of constituent honeybees [2]. Honeybees are one of several social biological systems that have so far frustrated attempts to clearly delineate a distinction between single organisms and groups of organisms [3]. Indeed, the honeybee colony exhibits so much large-scale integrity and responsivity that it has invited the description as a "superorganism" [4]. This coordination at many scales leads us to consider the role of cascade processes in the organization of honeybee colonies. We use multifractal analysis of individual honeybee activity as a means to demonstrate that both sources of multifractality, that is, equivalently, both entailments of cascade processes reveal the specific imprint of colony membership on individual honeybee activity. The multifractal dynamics of individual honeybee activity will emerge as a strong predictor of which of five colonies each individual honeybee belongs to.

II. SWARM COORDINATION: DECISION-MAKING AS A CASCADE

Swarm behavior reflects a remarkably flexible and distributed decision-making process that capitalizes on a decentralized organization but also on aggregation of information [5]. For instance, when a honeybee colony begins to outgrow its hive, scouts spread out widely to explore a vast range of options for the location of a new hive. Scouts return and share their information in terms of waggle dances that encourage other scouts to inspect new candidate areas. There do not appear to be social pressures acting on the honeybees through which one honeybee might influence another or conform to a group's preference. Rather, the honeybees arrive independently at their preference for a candidate site and explicitly vote, potentially with a waggle dance to second the original scouts' choices. Interestingly, swarm decision-making appears to depend on a minimum quorum of positive votes for a location and does not wait for unanimous endorsement. Hence, each scout may express her preference, but then the swarm will begin to act once members sense a quorum—the means of which quorum sensing remain controversial.

A. Multifractal evidence in honeybee movements consistent with cascade processes

This swarm-mediated sharing of information and executing a proposed plan reflects a sort of informational cascade in which coordination and interdependence rests on the rich diversity of relatively autonomous constituents [6]. This characterization of honeybee colonies and swarms as cascadelike is consistent with known aspects of honeybee-movement dynamics. For instance, the mathematical class of formalisms known as cascades can give rise specifically to power-law (i.e., fractal) scaling of probability distributions [7,8] and more generically to multifractal distributions best described by a variety of power laws [9–12]. Honeybee-movement dynamics exhibits at least two qualitatively different types of power-law forms: Levy statistics and long-range temporal correlations (also known as correlated random walks) [13,14].

B. Three sources of multifractality: Heavy-tailed Levy-like distributions, long-range linear correlations, and long-range correlations arising from nonlinear interactions across time

Levy statistics and long-term temporal correlations are two ostensibly separable mathematical expressions of fractal patterning: Levy statistics manifest in inverse power-law distributions—as well as Levy-like statistics that have heavy-

tailed distributions resembling inverse power laws [15]—in which probability diverges according to a negative power-law exponent between −1 and −3, and long-range temporal correlations often appear formalized in terms of fractionally integrated Gaussian noise [16]. Long-range correlations are in this case purely linear. It is certainly possible for one to occur in the absence of the other: Levy statistics may reflect the random, uncorrelated sequence of unrelated and occasionally extreme events [17], and long-range temporal correlations in Gaussian distributions will by definition fail to show heavy-tailed distributions. However, it is possible for developing distributions to blend heavy tails and long-range temporal statistics [16] or to transition between these extremes [12], and these hybrids are the simplest way to generate or to explain multifractal distributions. Further, long-range temporal correlations may lead inevitably to Levy statistics, but it remains unclear whether long-range temporal correlations explains the appearance of Levy statistics in honeybees [18].

However, there is a specific entailment of cascade processes presenting another possible source of multifractal distributions, namely, nonlinear interactions across time. An important distinction to make is that long-range linear temporal correlations typically associated with fractionally integrated Gaussian noise are a limiting case: fractionally integrated Gaussian noise is a specifically linear specification of monofractal temporal sequence. Here we are interested in long-range nonlinear correlations, i.e., temporal correlations insofar as they reflect the nonlinear phase relationships entailed by cascades [19–33]. Proper diagnosis of nonlinear interactions across time requires multifractal analysis [34]. Previous evidence of heavy tails in honeybee movements has also included monofractal fluctuation analysis and Fourier-based power-spectral analyses [13,14]. Both of these latter analyses are strictly monofractal analyses [35]. Perhaps one reason that temporal correlations have not accounted for Levy statistics in honeybee movements is that monofractal analysis is strictly linear and so not sufficiently generic to speak conclusively to the long-range correlations due to cascade-generated nonlinear interactions across time.

III. MULTIFRACTAL ANALYSIS TO IDENTIFY THE TWO CASCADE-DRIVEN PROPERTIES OF SPECIFIC COLONY

Essentially, heavy-tailed distributions and long-range correlations due to nonlinear interactions across time scale are two separately diagnosable mathematical entailments of a cascade model for the superorganismic coordination of decision-making. The present article does not seek to explain heavy-tailed statistics, but rather it will use multifractal analysis to quantify the colony-specific signature that cascade processes might impress upon the activity of individual honeybees. Because multifractal analysis is sensitive to both heavy-tailed distribution and to long-range correlations due to nonlinear interactions across time [36,37], multifractal analysis is uniquely suited to the task of quantifying both the degree of heavy-tailedness and the strength of long-range correlations due to nonlinear interactions across time.

At first glance, this double duty that we propose for multifractal analysis might seem to conflate the two separate entailments of cascade processes that the literature has sought to articulate as mathematically different—if blendable and ultimately related. However, using multifractal analysis in conjunction with surrogate data allows a subtle dissociation of the two types of multifractality: (1) multifractality due to heavy tails and (2) multifractality due to long-range correlations (i.e., nonlinear interactions across time scales). Surrogate data are simulated reconstructions of original observed data used, in nonlinear-dynamics research, to stand in for the null hypothesis that our observed data arise from strictly linear stochastic processes. For instance, whereas nonlinear phase relationships producing long-term correlations and whereas original sequence can be important for nonlinear stochastic processes, surrogate data embody the original data's linear properties (i.e., the original mean, variance, and autocorrelation) but in an arrangement that destroys any of the original sequence that might follow from nonlinearity [38,39]. Specifically, multifractal analysis estimates a multifractal spectrum whose width indicates the range of exponents (also known as "singularity strengths") for estimable power-law relationships across time scales. (Note: power laws are described as "singular" because of their scale-invariant property.) The width of the original series' multifractal spectrum w_{MF} is an ambiguous reflection of both the heaviness of tails in the series' distribution and the long-range correlations due to nonlinear interactions across time. Surrogate data can help to dissociate these two sources of multifractality with the application of multifractal analysis to surrogate series designed to preserve only the linear properties of the original series (i.e., mean, variance, and autocorrelation function). If there are long-range correlations due to nonlinear interactions across time in the original series, however, then there should be a significant difference of the original series' multifractal spectrum width from the multifractal spectrum widths for the surrogate series'. Hence, we can use a t-statistic comparing original spectrum width to surrogates' spectrum widths as a standardized difference statistic t_{MF} to quantify the degree of long-range correlations due to nonlinear interactions across scale. Taken together, both heavy-tailed distributions and long-range correlations due to nonlinear interactions across scales might together explain the subtle mixture of interdependence and individuality that makes the superorganism of the honeybee colony at once so robust but also so flexible as to challenge straightforward summary and delineation [5].

A. Exploring whether multifractal properties w_{MF} and t_{MF} for individual honeybees help indicate colony membership

We use w_{MF} and t_{MF} together in the same regression models to test whether these descriptions of individual honeybee behavior in fact predict colony membership. That is, rather than simply look for group effects on individual honeybees' movement patterns, we approach the potentially more challenging issue of beginning from the individual honeybee—free and indifferent to social conformity as it is—and attempt to read the multifractality of its activity for clues as to its colony membership. Neuroscientific evidence has already inspired mathematical modeling of neuronal coding within a single honeybee's nervous system that might contribute to the heavy-tailed distribution and long-range linear autocorrelation of honeybee-movement dynamics [40]. Hence, left to their own

individual devices, there may be enough multifractal diversity in a single honeybee's neural dynamics to generate heavy-tailed distributions—that is, enough multifractal structure at the neural level to specify heavy-tail-driven multifractal behavior at the scale of their eventual trajectories. However, the evidence of swarm behaviors such as quorum sensing entails a degree of interaction across scales of time and space that should translate as well to some echo of similar multifractality in honeybees of the same colony driven by long-range correlations due to nonlinear interactions across time. In a similar way that Gutierrez and Cabrera [40] presumed to "decode" experimental neuronal data for multifractal evidence of the corresponding heavy-tailed movement pattern, we now aim to decode experimental honeybee-movement data for multifractal evidence of colony membership.

B. Hypotheses

We show that both measures of cascade processes will serve as statistical signatures of colony-wide coordination that leave an imprint on individual honeybee behavior and that allow statistically assigning any given honeybee to its proper colony. Given that the degree of multifractality driven by heavy-tailed contributions might reflect the separate neural dynamics of individual honeybees, the strength of long-range correlations due to nonlinear interactions across time, i.e., t_{MF}, should emerge more clearly in a prediction of specific colony membership than it might serve a coarser distinction among colonies. In what follows, we present reanalysis of honeybee-movement data based strictly on time stamps logged when honeybees occupied a specific location within each of five colonies. We can draw a coarser distinction regarding whether the colony had or did not have an exterior-mesh enclosure surrounding the hive: two colonies had this enclosure and the other three did not. The t_{MF} of individual honeybee activity might predict the relatively generic presence or absence of a mesh enclosure in a logistic regression of this presence-absence dichotomous variable. A multinomial regression predicting the subtler distinction of membership in any of the five specific colonies brings into relief more robust contributions of both w_{MF} and t_{MF}. In sum, long-range correlations due to nonlinear interactions across time t_{MF} of honeybee movements never fail to predict some aspects of colony membership [40], but multifractality ω_{MF} encodes specific colony membership. These findings hold as well in the concurrent presence of various more straightforward estimates of magnitude from skewed distributions (e.g., mean, median, and maximum; first and third quartiles; whether for all values or only for values in the tail).

C. Description of the honeybee-movement dataset

The present work is a reanalysis of data originally reported elsewhere on logging time stamps of individual honeybees' exits from and entries to their colonies using radio-frequency identification (RFID) [41]. Experimenters augmented each colony's hive with a walkway to the hive's entrance. This walkway contained two RFID readers: one closer to the hive and one closer to the aperture of the walkway.

This reanalysis deals only with RFID time stamps for each honeybee. Despite the idealized possibility of inferring direction of flight, the RFID readers did not necessarily detect all honeybees at all times, and the walkway was also spacious enough to allow honeybees to reverse course. The present analysis simply deals with the time stamps irrespective of reader designation. This omission of reader designation essentially collapses the meaning of the RFID data to time stamps when the honeybee is in a region centered at the midpoint between the two readers. We only considered the time stamps in terms of the resulting interval series.

As the subsequent details on data analysis may illustrate, these data were not collected originally for multifractal analysis and are not ideal for these purposes. However, we approached this dataset as a means to test the robustness of the above logic regarding cascade coordination and specificity of multifractal properties to cascade structure. We did not test for multifractal structure in any series with fewer than 20 intervals. A common concern is "finite-size effects" on multifractal analysis, meaning that short series can produce spurious multifractal results, yielding an artifactually larger than zero multifractal spectrum width [32,33,42]. For the remainder of the series longer than 20 intervals, there was no finite-size effect on multifractal spectrum width. That is to say, there was no significant relationship between the number of intervals and the multifractal spectrum width—except in interaction terms indicating that a greater number of intervals diminished the effects of heavy-tailed distributional properties. The short samples and strong dilution of the sample with zero values should have made the test of multifractal indicators where we could generate nonzero estimates extremely unlikely to find a positive result. The presence of positive results in spite of the limitations of this dataset warrants further consideration.

IV. METHOD

A. Data collection

Tenczar *et al.* [41] attached RFID tags to 163 and 391 individual honeybees in each of two "experimental" colonies, colony 1 and colony 2, each bounded by a mesh enclosure (6 m wide × 20 m long × 3 m high; with total populations of 921 and 1051, respectively), as well as to 102, 119, and 369 individual honeybees in each of three "open" colonies, colony 3, colony 4, and colony 5 (with total populations of roughly 958, 932, and 979, respectively). The two former experimental colonies had mesh enclosures receiving *ad libitum* pollen, water, and 50% sucrose solution placed in feeders near the colony and replenished every day. Details of data collection can be found in [41]. Figure 1 shows four example series of intervals between RFID readings for four example honeybees.

B. Data analysis

1. Descriptive statistics

Data analysis involved first generating descriptive statistics on the skewed distributions of inter-reading intervals for each individual tagged honeybee (Fig. 2). Unsigned interval series are amenable to multifractal analysis [43,44]. Series length varied from 21 intervals at the minimum to 2246 intervals at the maximum, with first quartile, median, and third quartiles of

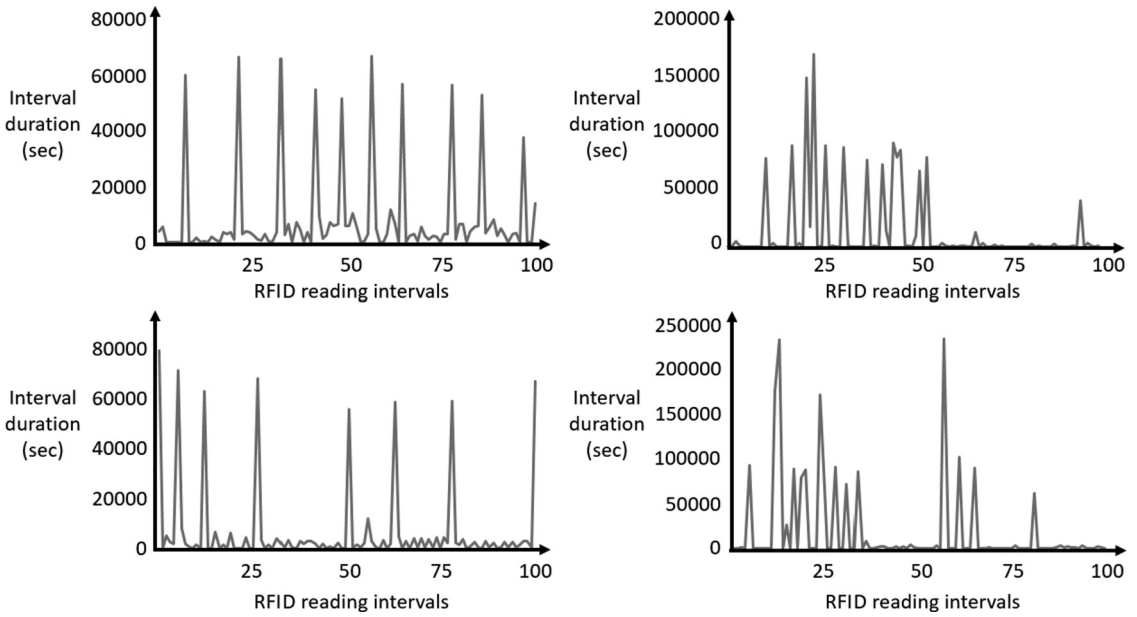

FIG. 1. Four example plots of RFID-reading interval series from four example honeybees. Original series lengths varied, but these plots depict only 100 successive intervals from each so as to show examples of the same length. All series depicted passed the augmented Dickey-Fuller test for stationarity, with nonstationarity rejected at $p < 0.05$.

150, 243, and 393, respectively. For quantifying magnitude of the entire distribution, we used median, mean, and maximum inter-reading intervals (I_{Median}, I_{Mean}, and I_{Max}, respectively). For quantifying the magnitude of only large intervals, we classified intervals as those greater than 30 000 s as long trips (LTs), and we used the median and mean of these intervals longer than 30 000 (I_{LTMedian} and I_{LTMean}, respectively). We did not use the maximum of these LT intervals because they were equivalent with the maximum of the entire distribution of intervals.

To generate a rough measure of temporal structure across the series of intervals, we computed the time intervals between each LT interval and computed descriptive statistics on these intervals-between-large-intervals: median, mean, and maximum of inter-LT intervals (B_{Median}, B_{Mean}, and B_{Max}, respectively).

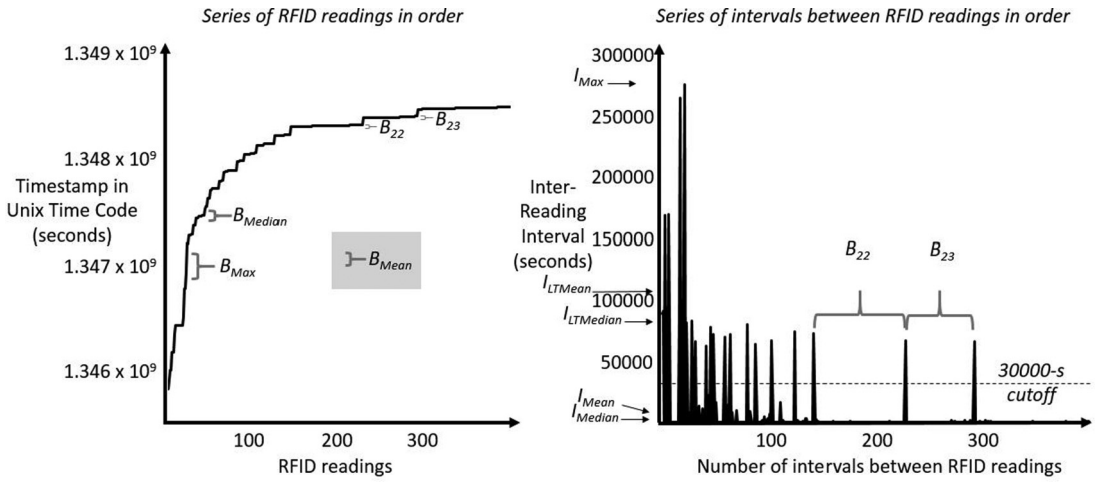

FIG. 2. Example plot of RFID-reading time stamp series for an individual honeybee (left panel) and of inter-reading intervals series for the same honeybee (right panel). Arrows indicate the location on the right panel's vertical axis of the median, mean, and maximum inter-reading interval (I_{Median}, I_{Mean}, and I_{Max}, respectively), as well as the median, mean, and maximum "long-trip" inter-reading interval (I_{LTMedian}, I_{LTMean}, and I_{LTMax}, respectively) describing the distribution of intervals above the 30 000-s cutoff shown by the dashed horizontal line. The left panel also includes brackets to indicate the intervals B between these long-trip intervals, specifically the median, the maximum, and, in the gray-shaded box inset, the mean (B_{Median}, B_{Mean}, and B_{Max}, respectively). To aid comparison, both panels show the 22nd and 23rd values of B (i.e., 85 708 and 83 884 seconds apart) on the RFID-reading domain (left panel) and on the inter-reading interval domain (right panel).

2. Multifractal analysis

We used Chhabra and Jensen's (CJ) [45] canonical "direct" algorithm for calculating the multifractal spectrum width w_{MF} that samples measurement series $u(t)$ at progressively larger scales. For each q, each estimated $\alpha(q)$ appears in the multifractal spectrum only when negative Shannon entropy of mass $\mu(q,L)$ scales with L according to the Hausdorff dimension $f(q)$, where

$$f[\alpha(q)] = -\lim_{N_j\to\infty} \frac{\sum_{i=1}^{N_j} \mu_{ij}(q,L_j)\ln[\mu_{ij}(q,L_j)]}{\ln N_j},$$

$$f[\alpha(q)] = \lim_{L_j\to 0} \frac{\sum_{i=1}^{N_j} \mu_{ij}(q,L_j)\ln[\mu_{ij}(q,L_j)]}{\ln L_j}, \quad (1)$$

and where the mass-weighted bin proportion scales with L as

$$\alpha(q) = -\lim_{N_j\to\infty} \frac{\sum_{i=1}^{N_j} \mu_{ij}(q,L_j)\ln[P_{ij}(L_j)]}{\ln N_j},$$

$$\alpha(q) = \lim_{L_j\to 0} \frac{\sum_{i=1}^{N_j} \mu_{ij}(q,L_j)\ln[P_{ij}(L_j)]}{\ln L_j}. \quad (2)$$

For $-10 \leqslant q \leqslant 10$, and including only linear relationships with correlation coefficient $r > 0.995$ for Eqs. (1) and (2), the downward-opening curve $(\alpha(q),f(q))$ is the multifractal spectrum. $\alpha_{\max}$-$\alpha_{\min}$ is the multifractal spectrum width w_{MF} according to the CJ algorithm. We used the CJ algorithm for these short series because, unlike other multifractal methods that use detrending, we were not certain that the short series would support the stable estimations of linear or polynomial trends or that the resulting residuals left over would be reliable estimates for fractal analysis. The CJ method relies only on local means and so does not require as much on the stability of linear or polynomial change.

(a) Calculating t_{MF} from comparison to iterated amplitude adjusted Fourier-transform (IAAFT) surrogates. 50 surrogates were produced according to the IAAFT procedure [39,46–48] for each original inter-reading interval series, using 1000 iterations. This IAAFT procedure generates surrogate data that preserves the linear properties of mean and variance by maintaining the original values of the series, and it preserves the autocorrelation while destroying any nonlinear phase relationship implicit in the original sequence. The first step of this procedure for any given series is to submit it to the Fourier transform that calculates, for every series, an amplitude spectrum expressing the size of oscillations over a wide range of frequencies and a phase spectrum that indicates the order in which these oscillations at each frequency first appear in the time series. Hence, the amplitude spectrum encodes information about the average temporal structure across many different time scales, corresponding to the autocorrelation function which was the third property of a linear stochastic process. The phase spectrum encodes sequence information which is a distinguishing feature only for stochastic processes of the nonlinear type. The IAAFT procedure thus stores the amplitude spectrum of the original series and it randomizes the phase spectrum to destroy any original sequence. Next, the IAAFT procedure computes an inverse-Fourier transform using the original preserved amplitude spectrum and the randomized phase spectrum. The inverse-Fourier procedure will project the preserved amplitude spectrum and randomized phase spectrum into a real-numbered series, but this projection is not necessarily distributed with the same mean and variance of the original series. To overcome this limitation, the IAAFT procedure concludes each iteration with an "amplitude-adjustment" step that rank orders the values of the inverse-Fourier series and replaces each value with rank-matched values of the original series. This amplitude-adjustment step concludes a single iteration, and IAAFT involves multiple iterations because amplitude adjustment will change small deviations in the amplitude spectrum of the resulting surrogate. Repeated iterations help to repeatedly inject the original series amplitude spectrum into the surrogate, strengthening the ability of the surrogate to represent the linear feature of the autocorrelation function. We calculated t_{MF} as the difference $[w_{\mathrm{MF}} - (\frac{1}{50})\sum_{i=1}^{50} w_{\mathrm{Surr}}(i))]$ divided by the standard error of w_{Surr}. Hence, positive or negative t_{MF} indicated wider or narrower, respectively, spectra than surrogates. We evaluated significance at the $p < 0.05$ level.

(b) Criteria for setting zero values. We submitted all series of inter-reading intervals of length greater than 20 intervals to multifractal analysis. For those inter-reading interval series of length 20 intervals or shorter, we automatically set w_{MF} and t_{MF} to zero. For those inter-reading interval series of length greater than 20 intervals that did not reveal any linear relationship for Eqs. (1) and (2), we automatically set these variables to "NaN" (not a number). Subsequent modeling converted NaNs to zeros without any change in the results.

3. Logistic regression

Logistic regression is a standard method for modeling the odds of a dichotomous (i.e., two-valued, noncontinuous) outcome in terms of a product of independent predictors. For any dichotomous outcome variable y, the individual probability p_i an individual i experiencing or exhibiting a dichotomous property or event 0 or 1 in the set of possible values for y is approximable by the average probability across the sample. We can express any proportion p_i in terms of odds $p_i/(1-p_i)$, and the logarithms of these odds are amenable to linearized regression. Hence, logistic regression models a dichotomous y in terms of n predictors $x_1,x_2,x_3,\ldots,x_{n-2},x_{n-1},x_n$ as follows:

$$\ln\left(\frac{p_i}{1-p_i}\right) = \beta_0 + \beta_1 x_1 + \beta_2 x_2 + \beta_3 x_3 + \cdots + \beta_{(n-2)}x_{(n-2)} + \beta_{(n-1)}x_{(n-1)} + \beta_n x_n + \varepsilon, \quad (3)$$

where β_0 and $\beta_1,\beta_2,\beta_3,\ldots,\beta_{n-2},\beta_{n-1},\beta_n$ are constants indicating the intercept (i.e., the proportion of outcome y when the predictors all equal zero) and the weights on contributions of predictors $x_1,x_2,x_3,\ldots,x_{n-2},x_{n-1},x_n$, respectively. The size and sign of the coefficients $\beta_1,\beta_2,\beta_3,\ldots,\beta_{n-2},\beta_{n-1},\beta_n$ indicate the strength and direction of the effect of $x_1,x_2,x_3,\ldots,x_{n-2},x_{n-1},x_n$, respectively, on the logarithmic odds of y. Exponentiating $\beta_1,\beta_2,\beta_3,\ldots,\beta_{n-2},\beta_{n-1},\beta_n$ produces odds ratios indicating how many times a unit increase of $x_1,x_2,x_3,\ldots,x_{n-2},x_{n-1},x_n$ increases the odds of y [49].

4. Multinomial regression

Multinomial regression generalizes logistic regression to suit modeling a categorical variable z with $k > 2$ values. Whereas logistic regression allows regressing y on a set of

predictors in one equation, multinomial regression treats a kth value of z as a baseline and models $k-1$ equations of similar form to Eq. (4) that model the logarithmic odds that each jth individual case embodies property or event $1,2,\ldots,k-2,k-1$ and not baseline property or event k. Hence, the regression equations are as follows:

$$\begin{aligned}
\ln\left(\frac{p_{1j}}{p_{kj}}\right) &= \beta_{10}+\beta_{11}x_{11}+\beta_{12}x_{12}+\beta_{13}x_{13}+\cdots+\beta_{1(n-2)}x_{1(n-2)}+\beta_{1(n-1)}x_{1(n-1)}+\beta_{1n}x_{1n}+\varepsilon_1,\\
\ln\left(\frac{p_{2j}}{p_{kj}}\right) &= \beta_{20}+\beta_{21}x_{21}+\beta_{22}x_{22}+\beta_{23}x_{23}+\cdots+\beta_{2(n-2)}x_{2(n-2)}+\beta_{2(n-1)}x_{2(n-1)}+\beta_{2n}x_{2n}+\varepsilon_2,\ldots,\\
\ln\left(\frac{p_{(k-2)j}}{p_{kj}}\right) &= \beta_{(k-2)0}+\beta_{(k-2)1}x_{(k-2)1}+\beta_{(k-2)2}x_{(k-2)2}+\beta_{(k-2)3}x_{(k-2)3}+\cdots+\beta_{(k-2)(n-2)}x_{(k-2)(n-2)}+\beta_{(k-2)(n-1)}x_{(k-2)(n-1)}\\
&\quad+\beta_{(k-2)n}x_{(k-2)n}+\varepsilon_{(k-2)},\\
\ln\left(\frac{p_{(k-1)j}}{p_{kj}}\right) &= \beta_{(k-1)0}+\beta_{(k-1)1}x_{(k-1)1}+\beta_{(k-1)2}x_{(k-1)2}+\beta_{(k-1)3}x_{(k-1)3}+\cdots+\beta_{(k-1)(n-2)}x_{(k-1)(n-2)}+\beta_{(k-1)(n-1)}x_{(k-1)(n-1)}\\
&\quad+\beta_{(k-1)n}x_{(k-1)n}+\varepsilon_{(k-1)},
\end{aligned} \tag{4}$$

where for $1\leqslant v\leqslant k-1,\beta_0$ and $\beta_{v1},\beta_{v2},\beta_{v3},\ldots,\beta_{v(n-2)}$, $\beta_{v(n-1)}$, β_{vn} are constants indicating the intercept (i.e., the proportion of outcome y when the predictors all equal zero) and the weights on contributions of predictors $x_{v1},x_{v2},x_{v3},\ldots,x_{v(n-2)},x_{v(n-1)}$, x_{vn}, respectively. The size and sign of the coefficients $\beta_{v1},\beta_{v2},\beta_{v3},\ldots,\beta_{v(n-2)},\beta_{v(n-1)}$, β_{vn} indicate the strength and direction of the effect of $x_{v1},x_{v2},x_{v3},\ldots,x_{v(n-2)},x_{v(n-1)}$, x_{vn}, respectively, on the logarithmic odds of z taking the value of w rather than of k [50].

V. RESULTS

A. Multifractal results on inter-reading intervals

362 honeybees had inter-reading interval series of length 20 or less and so were never submitted to multifractal analysis. 89.20% of the remaining series showed significant augmented Dickey-Fuller tests for unit roots [51], indicating that most of the series were stationary. 213 honeybees failed to yield linear relationships according to Eqs. (1) and (2), with colonies 1 and 2 having 20.48% and 15.86%, respectively, and with colonies 3, 4, and 5 having 17.47%, 32.77%, and 16.22%, respectively. All such failures were encoded as having $w_{\mathrm{MF}}=0$.

Of the remaining 574 series, 370 had multifractal spectra with widths significantly different from those of their corresponding surrogates (e.g., Fig. 5). In other words, of honeybees that generated sufficiently long series of and sufficiently stable relationships for Eqs. (1) and (2), 64.46% of these honeybees exhibited long-range correlations due to nonlinear interactions across scales through their inter-reading intervals. It remains in the next sections to determine whether or not this information from less than half of the total recorded honeybees is enough to predict colony membership even with so many zeros in the sample diluting the multifractal information.

As suggested by Fig. 5, the left side of the multifractal spectrum (i.e., for $q>0$) was often the more stable portion of estimates from the multifractal algorithm. Our use of an $r>0.95$ cutoff for estimating both $\alpha(q)$ and $f(q)$ simply made it less likely that our estimates would include the less stable right side of the multifractal spectrum. This instability for negative q is a known constraint for all "box-counting" algorithms like Chhabra and Jensen's [45] that depend on tiling a measurement with nonoverlapping bins from the beginning of a measurement [52–59], but many empirical examples suggest that the left side of the multifractal spectrum may support the better prediction of structural change for natural systems, ranging from the vast scales of solar radiation [60] and atmospheric flows [61,62], to the smaller scales of soil composition [63], magnetic particles [64], and battery voltage [65]; and as well to the medium scales of social organisms pooling and competing for resources [66].

A related concern regarding finite-size effects on multifractal estimates is that, for short series, the moments of large q's may cause Eqs. (1) and (2) to diverge [67,68]. To resolve this concern, we include plots of Eqs. (1) and (2) for the integer values of q for the first quartile of interval-series lengths, i.e., length $N_{\mathrm{ints}}=150$. Figures 3 and 4 depict the plotted relations for Eqs. (1) and (2), respectively, for an example series of length $N_{\mathrm{ints}}=150$. As noted above, we only included values of q for the estimation of multifractal spectra for which both Eq. (1) and Eq. (2) supported linear relations with correlations greater than $r=0.995$. Hence, this $N_{\mathrm{inits}}=150$ series certainly failed to support many of the tested values of q from -10 to 10, inclusive, but nonetheless, in the interest of ensuring that our multifractal spectra were conservatively estimated, we included the depicted five values of q for which the relations in Eqs. (1) and (2) for corresponding q were demonstrably linear. All relations in Eq. (1) for which either Eq. (1) or Eq. (2) did not exhibit an $r>0.995$ relationship were omitted from the calculation of w_{MF}.

B. Multifractality of inter-reading intervals for single honeybees distinguishes presence or absence of mesh boundary

A logistic regression modeled whether or not honeybees belonged to an experimental colony with an exterior-mesh boundary. Predictors initially included the mean, median, and maximum inter-reading intervals (i.e., I_{Median}, I_{Mean},

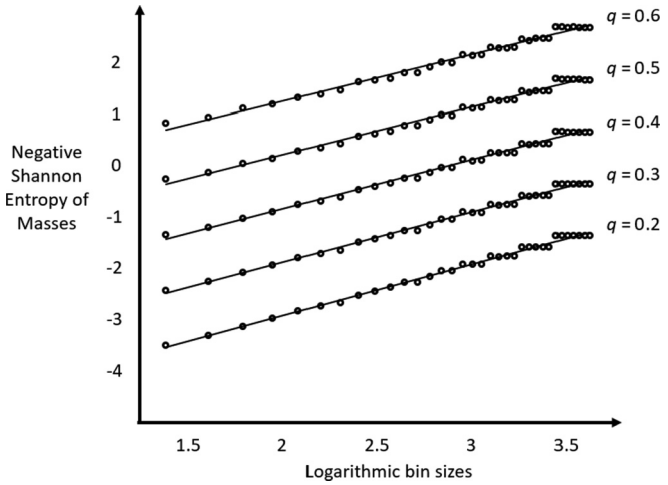

FIG. 3. Example plot of relations between negative Shannon entropy of bin masses $\mu(q,L)$ and logarithmic bin size L in Eq. (3) for an example interval series of length 150. This depicts all values of q that passed our $r > 0.995$ criterion for inclusion into the multifractal spectrum we used for calculating w_{MF}. Plots for different values of q appear separated by vertical constant only to aid visibility. All relations in Eq. (1) for which either Eq. (1) or Eq. (2) for corresponding q did not exhibit a $r > 0.995$ relationship were omitted from the calculation of w_{MF}.

and I_{Max}) as well as the multifractal spectrum width w_{MF} and the t-statistic t_{MF} comparing w_{MF} to the widths of 50 IAAFT surrogates. The logistic-regression equation related the logarithmic odds of each ith bee belonging to a colony with a mesh boundary M (i.e., the presence or absence of a mesh boundary encoded as $M = 1$ or 0, respectively) to a set

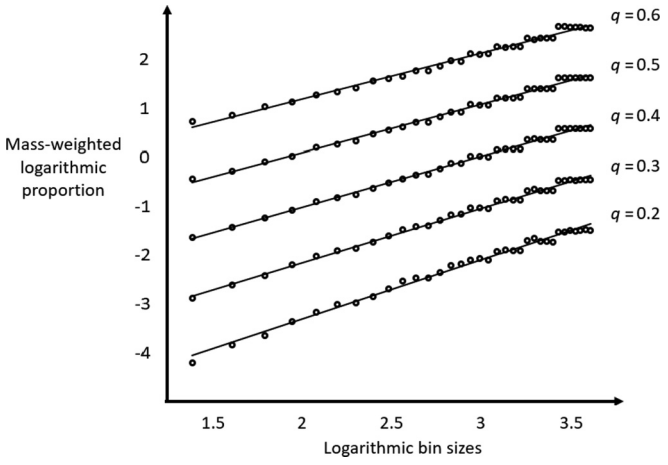

FIG. 4. Example plot of relations between mass $\mu(q,L)$-weighted bin proportion and logarithmic bin size L in Eq. (2) for an example interval series of length 150. This depicts all values of q that passed our $r > 0.995$ criterion for inclusion into the multifractal spectrum we used for calculating w_{MF}. Plots for different values of q appear separated by vertical constant only to aid visibility. All relations in Eq. (2) for which either Eq. (1) or Eq. (2) for corresponding q did not exhibit a $r > 0.995$ relationship were omitted from the calculation of w_{MF}.

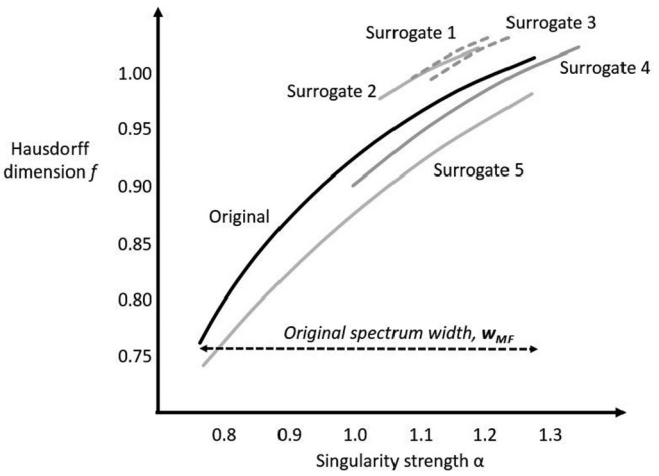

FIG. 5. Example plot of multifractal spectra showing the multifractal spectrum for the original inter-reading interval series shown in the right panel of Fig. 2 (solid black) as well as for five IAAFT surrogates preserving the same values as the original and its linear autocorrelation (gray lines, dashed or solid or light to distinguish them from one another when overlapping). The width of the original series' multifractal spectrum w_{MF} is 0.5134 indicated by the dashed black arrow at the bottom of the plot. Surrogates generally had narrower multifractal spectra, with surrogates 1–4 having widths 0.1505, 0.1224, 0.1153, and 0.3465. Surrogate 5 had the closest spectrum width (0.5026) to that for the original.

of predictors as follows:

$$\ln\left(\frac{p_i}{1-p_i}\right) = \beta_{\mathrm{Intercept}} + \beta_1 I_{\mathrm{Median}} + \beta_2 I_{\mathrm{Mean}} + \beta_3 I_{\mathrm{Max}} + \beta_4 w_{\mathrm{MF}} + \beta_5 t_{\mathrm{MF}} + \varepsilon. \quad (5)$$

All effects were significant including w_{MF} and t_{MF} in this version of the model (Table I), with estimated coefficients β_4 and β_5 entailing an odds ratio of $e^{-0.42} = 0.66$ for w_{MF} and $e^{0.03} = 1.03$ for t_{MF}, respectively. That is, a unit increase in multifractal spectrum width makes it a third less likely and that a unit increase in t_{MF} makes it 1.03 times more likely that the honeybee belongs to a colony with an exterior mesh.

Given the small size of the dataset, it is important to test this effect of long-range temporal correlations against a yet longer list of simpler descriptive statistics. We hope to guard against the possibility that the earlier result is not simply a result of "data massaging" or of contrived models small enough to

TABLE I. Coefficients for logistic regression testing aspects of inter-reading intervals for distinguishing experimental colonies with from open colonies without mesh enclosures—basic descriptives and multifractal statistics.

Predictor	B	SE	p
Intercept	0.80	0.14	<0.0001
I_{Median}	-5.90×10^{-6}	6.98×10^{-6}	0.40
I_{Mean}	7.55×10^{-6}	6.08×10^{-6}	0.21
I_{Max}	-4.70×10^{-6}	6.62×10^{-7}	<0.0001
w_{MF}	−0.42	0.23	0.06
t_{MF}	0.03	0.01	<0.05

TABLE II. Coefficients for logistic regression testing aspects of inter-reading intervals for distinguishing experimental colonies with and open colonies without mesh enclosures—basic descriptives and multifractal statistics but also including descriptive statistics long-trip intervals and intervals between long trips.

Predictor	*B*	*SE*	*p*
Intercept	1.30	0.44	<0.0001
I_{Median}	-4.05×10^{-6}	8.43×10^{-6}	0.63
I_{Mean}	1.06×10^{-5}	9.51×10^{-6}	0.27
I_{Max}	-8.05×10^{-6}	2.05×10^{-6}	<0.0001
w_{MF}	−0.27	0.22	0.21
t_{MF}	0.03	0.01	<0.05
I_{LTMedian}	-3.09×10^{-7}	9.08×10^{-6}	0.97
I_{LTMean}	1.21×10^{-5}	1.14×10^{-5}	0.29
B_{Median}	3.29×10^{-7}	1.07×10^{-5}	0.98
B_{Mean}	-2.13×10^{-5}	1.26×10^{-5}	0.09
B_{Max}	5.77×10^{-6}	2.22×10^{-6}	<0.01

show a potentially desired effect. Table II reports an elaborated logistic regression that incorporates both the descriptive statistics on intervals of arbitrary length (i.e., $I_{\text{LTMedian}}, I_{\text{LTMean}}$) and the descriptive statistics on intervals between arbitrarily long intervals (B_{Median}, B_{Mean}, and B_{Max}). This elaborated logistic-regression equation related logarithmic odds of each ith bee belonging to a colony with a mesh boundary M (i.e., the presence or absence of a mesh boundary encoded as $M = 1$ or 0, respectively) to a set of predictors as follows:

$$\ln\left(\frac{p_i}{1-p_i}\right) = \beta_{\text{Intercept}} + \beta_1 I_{\text{Median}} + \beta_2 I_{\text{Mean}} + \beta_3 I_{\text{Max}} + \beta_4 w_{\text{MF}} + \beta_5 t_{\text{MF}} + \beta_6 I_{\text{LTMedian}} + \beta_7 I_{\text{LTMean}} + \beta_8 B_{\text{Median}} + \beta_9 B_{\text{Mean}} + \beta_{10} B_{\text{Max}} + \varepsilon. \quad (6)$$

The inclusion of each new effect individually improves model fit, but once all of these new effects appear in the model, only B_{Max} contributes significantly to predicting the presence or absence of an exterior-mesh boundary, with an odds ratio close to but just less than 1.

The effect $w_{\text{MF}}(\beta_4 = -0.27)$ is much weaker than in the previous model, indicating that the effect of multifractal spectrum width is less important than simpler descriptive statistics. However, the significant effect of t_{MF} that appeared in the reduced model in Table I remains stable ($\beta_4 = 0.03$) and remains significant.

Hence, we hope to have shown that the results are quite stable across multiple models and so multiple perspectives as to what other predictors might be relevant. Various alternate versions of this logistic regression support the same pattern of significance for w_{MF} and t_{MF}. For instance, adding the first and third quartiles for the intervals and for the long-term intervals does not change the pattern of significance. In short, given all of the limitations of estimating w_{MF} and t_{MF} under these small-sample constraints, these multifractal measures both show robust significant contributions to identifying whether or not honeybees belong to experimental colonies.

C. Multinomial regression predicting to specific colony indicates significant effect both of long-range correlations due to nonlinear interactions across time t_{MF} and of heavy-tailedness w_{MF}

A multinomial regression including all terms from the logistic regression in Table II aimed to test whether these terms might distinguish not simply between the presence or absence of an exterior-mesh boundary but, more specifically, distinguish the specific colonies to which the honeybees belonged. That is, given the five colonies, the multinomial regression comprised four equations modeling the logarithmic odds of each ith bee belonging to colony $1 \leqslant v \leqslant 5, v \neq 3$ rather than colony 3 of the following form:

$$\ln\left(\frac{p_{vi}}{p3_i}\right) = \beta_{v\text{Intercept}} + \beta_{v1} I_{v\text{Median}} + \beta_{v2} I_{v\text{Mean}} + \beta_{v3} I_{v\text{Max}} + \beta_{v4} w_{v\text{MF}} + \beta_{v5} t_{v\text{MF}} + \beta_{v6} I_{v\text{LTMedian}} + \beta_{v7} I_{v\text{LTMean}} + \beta_{v8} B_{v\text{Median}} + \beta_{v9} B_{v\text{Mean}} + \beta_{v10} B_{v\text{Max}} + \varepsilon_v. \quad (7)$$

We selected colony 3 as the control only because it was the first of the open colonies, and using this control case allows comparison of two experimental colonies as well as two open colonies. Most notably, the strongest predictors serving to distinguish across all the specific colony memberships were w_{MF} and t_{MF}. Hence, specific combinations of the multifractal spectrum width and the difference of this width from corresponding surrogates significantly improve prediction of which of four colonies besides colony 1 an individual honeybee might belong to. This finding indicates that, above and beyond simpler descriptive statistics, both long-range correlations due to nonlinear interactions across time t_{MF} and all remaining contributions of heavy-tailedness to w_{MF} may serve as a statistical trace of colony membership left in the inter-reading intervals of individual honeybees (Table III).

All various alternate versions as tested by the logistic regression above support the same pattern of significance for w_{MF} and t_{MF} in this multinomial regression.

D. Testing finite-size effects and finding only that longer series diminish effects of heavy-tailed distributional properties

The primary concern of finite-size effects on the multifractal spectrum is that overly short series might give rise to artifactually wide multifractal spectra, indicating only an "illusory" sort of multifractality. There was no clear relationship between multifractal spectrum width and series length N_{ints}. These two quantities bore a linear correlation close to zero, specifically, $r = 0.03$. We ran a linear regression model to test how any effects of series length might appear when fitting the covariates representing the heavy-tailed distributional properties of the intervals, i.e., I_{Median}, I_{Mean}, and I_{Max}, as well as the first and third quartiles of the intervals I_{q1} and I_{q3}, respectively. Table IV shows the coefficients from a model that only tests main effects. In these results, there was no main effect for N_{ints}, I_{Mean}, or I_{q3}. There were only main effects for I_{Median}, I_{Max}, and I_{q1}. Hence, there was no main effect of series length on multifractal width. A second linear regression model included all of the same effects as in the first model, as well

TABLE III. Coefficients for multinomial regression testing aspects of inter-reading intervals for distinguishing colonies 1, 2, 4, and 5 as compared to colony 3—including all coefficients for predictors in Table II in columns corresponding to colony.

	Colonies other than colony 3			
Predictor	Colony 1	Colony 2	Colony 4	Colony 5
Intercept	0.29^{***}	2.86^{***}	-0.27^{***}	1.45^{***}
	(3.08×10^{-9})	(8.30×10^{-10})	(7.73×10^{-10})	(1.02×10^{-9})
I_{Median}	-7.78×10^{-5}	7.98×10^{-6}	1.26×10^{-6}	$2.45 \times 10^{-5*}$
	(6.35×10^{-5})	(1.28×10^{-5})	(1.32×10^{-4})	(1.37×10^{-5})
I_{Mean}	2.96×10^{-6}	-3.69×10^{-6}	-5.44×10^{-6}	$-2.77 \times 10^{-5**}$
	(1.27×10^{-5})	(1.12×10^{-5})	(1.12×10^{-5})	(1.03×10^{-5})
I_{Max}	$-4.02 \times 10^{-6*}$	$1.10 \times 10^{-5***}$	$-6.14 \times 10^{-6*}$	-2.19×10^{-6}
	(2.26×10^{-6})	(2.54×10^{-6})	(2.65×10^{-6})	(1.87×10^{-6})
w_{MF}	-0.03^{***}	-0.29^{***}	-0.59^{***}	-0.07^{***}
	(4.43×10^{-9})	(1.50×10^{-9})	(4.34×10^{-10})	(1.55×10^{-9})
t_{MF}	0.01^{***}	0.01^{***}	-0.06^{***}	-0.02^{***}
	(2.79×10^{-8})	(1.24×10^{-8})	(1.96×10^{-9})	(9.26×10^{-9})
I_{LTMedian}	$-3.61 \times 10^{-5**}$	$-2.43 \times 10^{-5*}$	-1.46×10^{-5}	$-3.03 \times 10^{-5**}$
	(1.39×10^{-5})	(1.31×10^{-5})	(1.31×10^{-5})	(1.26×10^{-5})
I_{LTMean}	$3.96 \times 10^{-5**}$	$4.36 \times 10^{-5**}$	$3.58 \times 10^{-5*}$	$2.88 \times 10^{-5*}$
	(1.63×10^{-5})	(1.61×10^{-5})	(1.63×10^{-5})	(1.44×10^{-5})
B_{Median}	$3.26 \times 10^{-5*}$	$2.43 \times 10^{-5*}$	1.47×10^{-5}	$2.25 \times 10^{-5*}$
	(1.47×10^{-5})	(1.41×10^{-6})	(1.31×10^{-5})	(1.28×10^{-5})
B_{Mean}	$-3.67 \times 10^{-5*}$	$-5.03 \times 10^{-5**}$	$-3.16 \times 10^{-5*}$	-1.86×10^{-5}
	(1.66×10^{-5})	(1.67×10^{-6})	(1.49×10^{-5})	(1.45×10^{-5})
B_{Max}	4.42×10^{-6}	$9.45 \times 10^{-6**}$	$7.86 \times 10^{-6**}$	2.13×10^{-6}
	(2.72×10^{-6})	(2.89×10^{-6})	(2.85×10^{-6})	(2.29×10^{-6})

(*Note*. Standard errors in parentheses; *denotes $p < 0.05$; **denotes $p < 0.01$; ***denotes $p < 0.0001$.)

as interactions between N_{ints} and each of the distributional properties I_{Median}, I_{Mean}, I_{Max}, I_{q1}, and I_{q3}. Table V shows the coefficients from this second model. This second model yielded all significant effects except for a main effect of N_{ints}. The interactions of N_{ints} and each of the distributional properties I_{Median}, I_{Mean}, I_{Max}, I_{q1}, and I_{q3} all had the opposite sign from effects of the distributional properties I_{Median}, I_{Mean}, I_{Max}, I_{q1}, and I_{q3}. That is to say, the only effect of interval-series length is that longer series have multifractal spectrum widths less dependent on distributional properties. There is no evidence that shorter series yield illusory multifractality, that is, artifactually wider multifractal spectra. On the contrary, there is only evidence that shorter series are more likely to yield results consistent with heavy-tailed distributional properties, i.e., that shorter series are less likely to have significantly large t_{MF}.

TABLE IV. Coefficients for linear regression model of w_{MF} testing for effects of interval-series length N_{ints} as well as distributional properties of intervals, i.e., I_{Median}, I_{Mean}, and I_{Max}, as well as the first and third quartiles of the intervals I_{q1} and I_{q3}, respectively.

Predictor	*B*	*SE*	*p*
Intercept	0.48	0.08	<0.0001
N_{ints}	1.56×10^{-4}	1.24×10^{-4}	0.21
I_{Median}	-3.12×10^{-4}	3.25×10^{-5}	<0.0001
I_{Mean}	7.81×10^{-6}	5.48×10^{-6}	0.15
I_{Max}	-4.60×10^{-7}	2.20×10^{-7}	<0.05
I_{q1}	2.66×10^{-3}	2.68×10^{-4}	<0.0001
I_{q3}	6.70×10^{-6}	3.45×10^{-6}	0.05

VI. DISCUSSION

We have used the honeybee colony as a model system and multifractal modeling as a technique for modeling the cascadelike properties of five honeybee colonies. The different sources of multifractality in the measured series predict the type of colony to which an individual honeybee belongs.

TABLE V. Coefficients for linear regression of w_{MF} testing for effects of interval-series length N_{ints}, all other effects included in Table IV, and interactions of N_{ints} with all distributional properties of intervals, i.e., I_{Median}, I_{Mean}, and I_{Max}, as well as the first and third quartiles of the intervals I_{q1} and I_{q3}, respectively.

Predictor	*B*	*SE*	*p*
Intercept	0.76	0.09	<0.0001
N_{ints}	-5.20×10^{-5}	1.94×10^{-4}	0.79
I_{Median}	-4.29×10^{-4}	4.07×10^{-5}	<0.0001
I_{Mean}	2.18×10^{-5}	6.64×10^{-6}	<0.01
I_{Max}	-6.64×10^{-7}	3.36×10^{-7}	<0.05
I_{q1}	3.14×10^{-3}	3.03×10^{-4}	<0.0001
I_{q3}	1.81×10^{-5}	5.78×10^{-6}	<0.01
$N_{\text{ints}} \times I_{\text{Median}}$	2.32×10^{-6}	4.63×10^{-7}	<0.0001
$N_{\text{ints}} \times I_{\text{Mean}}$	-2.17×10^{-7}	5.18×10^{-8}	<0.0001
$N_{\text{ints}} \times I_{\text{Max}}$	2.38×10^{-9}	1.02×10^{-9}	<0.05
$N_{\text{ints}} \times I_{q1}$	-8.42×10^{-6}	3.38×10^{-6}	<0.05
$N_{\text{ints}} \times I_{q3}$	-3.47×10^{-7}	8.87×10^{-8}	<0.001

We found specifically that multifractality due to long-range correlations associated with nonlinear interactions across time was a good predictor of whether or not a colony operated within a mesh enclosure as well as a good predictor of membership in a specific colony. We also found that the heavy-tail-driven multifractality supported the more subtle distinction regarding individual colony. This finding aligns with previous research finding that multifractal signatures of long-range correlations due to nonlinear interactions of time spread readily through coordinations both between an individual organism with a task environment [69], as well as among multiple components of the human movement system [70–72]. That is only to say that the present findings may not reflect features unique to honeybees, and rather, biological coordinations appearing in different species can exhibit similar multifractal hallmarks of cascade organization that, in turn, predict different coordination patterns.

ACKNOWLEDGMENTS

N.S.C. and D.G.K.-S. acknowledge the generous support of Grinnell College's Mentored Advanced Project Program.

[1] L. J. Moore and M. Kosut, *Buzz: Urban Beekeeping and the Power of the Bee* (NYU Press, New York, 2013).
[2] J. C. Biesmeijer and T. D. Seeley, Behav. Ecol. Sociobiol. **59**, 133 (2005).
[3] J. Wilson, Philos. Sci. **67**, S301 (2000).
[4] T. D. Seeley, Am. Sci. **77**, 546 (1989).
[5] T. D. Seeley, P. K. Visscher, and K. M. Passino, Am. Sci. **94**, 220 (2006).
[6] C. List, C. Elsholtz, and T. D. Seeley, Philos. Trans. R. Soc. B **364**, 755 (2009).
[7] H. J. Jensen, *Self-Organized Criticality: Emergent Complex Behavior in Physical and Biological Systems* (Cambridge University Press, Cambridge, UK, 1998).
[8] D. L. Turcotte, B. D. Malamud, F. Guzzetti, and P. Reichenbach, Proc. Natl. Acad. Sci. USA **99**, 2530 (2002).
[9] B. B. Mandelbrot, J. Fluid Mech. **62**, 331 (1974).
[10] D. Schertzer and S. Lovejoy, Physicochem. Hydrodyn. **6**, 623 (1985).
[11] T. C. Halsey, M. H. Jensen, L. P. Kadanoff, I. I. Procaccia, and B. I. Shraiman, Phys. Rev. A **33**, 1141 (1986).
[12] M. F. Shlesigner, G. M. Zaslavsky, and J. Klafter, Nature (London) **363**, 31 (1993).
[13] A. M. Reynolds, A. D. Smith, D. R. Reynolds, N. L. Carreck, and J. L. Osborne, J. Exp. Biol. **210**, 3763 (2007).
[14] A. M. Reynolds, A. D. Smith, R. Menzel, U. Greggers, D. R. Reynolds, and J. R. Riley, Ecology **88**, 1955 (2007).
[15] D. W. Sims *et al.*, Nature (London) **451**, 1098 (2008).
[16] N. Scafetta and B. J. West, Complexity **10**, 51 (2005).
[17] S. Gheorghiu and M.-O. Coppens, Proc. Natl. Acad. Sci. USA **101**, 15852 (2004).
[18] A. M. Reynolds, J. R. Soc. Interface **7**, 1753 (2010).
[19] Y.-Y. Tsai, M.-C. Chang, and L. I, Phys. Rev. E **86**, 045402(R) (2012).
[20] D. Koga, A. C.-L. Chian, R. A. Miranda, and E. L. Rempel, Phys. Rev. E **75**, 046401 (2007).
[21] A. R. Osborne, Phys. Rev. E **52**, 1105 (1995).
[22] H. S. Harrison, D. G. Kelty-Stephen, D. V. Vaz, and C. F. Michaels, Phys. Rev. E **89**, 060903(R) (2014).
[23] A. Naert, R. Friedrich, and J. Peinke, Phys. Rev. E **56**, 6719 (1997).
[24] P. D. Ditlevsen and I. A. Mogensen, Phys. Rev. E **53**, 4785 (1996).
[25] R. C. Hogan and J. N. Cuzzi, Phys. Rev. E **75**, 056305 (2007).
[26] D. Biskamp, Phys. Rev. E **50**, 2702 (1994).
[27] V. Carbone, Phys. Rev. E **50**, R671(R) (1994).
[28] X. Qiu, L. Ding, Y. Huang, M. Chen, Z. Lu, Y. Liu, and Q. Zhou, Phys. Rev. E **93**, 062226 (2016).
[29] E. Leveque and Z. S. She, Phys. Rev. E **55**, 2789 (1997).
[30] V. M. Uritsky, A. Pouquet, D. Rosenberg, P. D. Mininni, and E. F. Donovan, Phys. Rev. E **82**, 056326 (2010).
[31] I. Nainville, A. Lemarchand, and J.-P. Badiali, Phys. Rev. E **53**, 2537 (1996).
[32] S. Drozdz, J. Kwapien, P. Oswiecimka, and R. Rak, Europhys. Lett. **88**, 60003 (2009).
[33] W.-X. Zhou, Chaos, Solitons Fractals, **45**, 147 (2012).
[34] E. A. F. Ihlen and B. Vereijken, J. Exp. Psychol. Gen. **139**, 436 (2010).
[35] A. Eke, P. Herman, L. Kocsis, and L. R. Kozak, Physiol. Meas. **23**, R1 (2002).
[36] J. W. Kantelhardt, S. A. Zschiegner, E. Koscielny-Bunde, S. Havlin, A. Bunde, and H. E. Stanley, Physica A **316**, 87 (2002).
[37] Z. R. Struzik, in *The Application of Econophysics*, edited by H. Takayasu (Springer, Tokyo, 2004).
[38] J. Theiler, S. Eubank, A. Longtin, B. Galdrikian, and J. D. Farmer, Physica D **58**, 77 (1992).
[39] T. Schreiber and A. Schmitz, Phys. Rev. Lett. **77**, 635 (1996).
[40] E. D. Gutierrez and J. L. Cabrera, Sci. Rep. **5**, 18009 (2015).
[41] P. Tenczar, C. C. Lutz, V. D. Rao, N. Goldenfeld, and G. E. Robinson, Animal Behav. **95**, 41 (2014).
[42] Z.-Q. Jiang and W.-X. Zhou, Physica A **387**, 3605 (2008).
[43] J. W. Kantelhardt, Y. Ashkenazy, P. Ch. Ivanov, A. Bunde, S. Havlin, T. Penzel, J.-H. Peter, and H. E. Stanley, Phys. Rev. E **65**, 051908 (2002).
[44] D. G. Kelty-Stephen, L. A. Stirling, and L. A. Lipsitz, Psychol. Assess. **28**, 171 (2016).
[45] A. B. Chhabra and R. V. Jensen, Phys. Rev. Lett. **62**, 1327 (1989).
[46] C. Rath and I. Laut, Phys. Rev. E **92**, 040902(R) (2015).
[47] N. P. Subramaniyam and J. Hyttinen, Phys. Rev. E **91**, 022927 (2015).
[48] D. Iatsenko, P. V. E. McClintock, and A. Stefanovska, Phys. Rev. E **92**, 032916 (2015).
[49] J. D. Singer and J. B. Willett, *Applied Longitudinal Data Analysis: Modeling Change and Event Occurrence* (Oxford University Press, New York, 2003).
[50] D. Hosmer and S. Lemeshow, *Applied Logistic Regression* (Wiley, New York, 2000).
[51] A. Banerjee, J. J. Dolado, J. W. Galbraith, and D. F. Hendry, *Cointegration, Error Correction and the Econometric Analysis of Non-Stationary Data* (Oxford University Press, Oxford, 1993).

[52] C. Rosales and C. Meneveau, Phys. Rev. E **78**, 016313 (2008).
[53] M. Alber and J. Peinke, Phys. Rev. E **57**, 5489 (1998).
[54] R. Blumenfeld and A. Aharony, Phys. Rev. Lett. **62**, 2977 (1989).
[55] C. Meneveau and K. R. Sreenivasan, Nucl. Phys. B **2**, 49 (1987).
[56] R. Pastor-Satorras and R. H. Riedi, J. Phys. A: Math. Gen. **29**, L391 (1996).
[57] T. C. Halsey, K. Honda, and B. Duplantier, J. Stat. Phys. **85**, 681 (1996).
[58] F. P. Agterberg, in *Geologic Modeling and Simulation*, edited by D. F. Merriam and J. C. Davis (Springer, New York, 2001).
[59] S. G. De Bartolo, S. Gabriele, and R. Gaudio, Hydrol. Earth Syst. Sci. **4**, 105 (2000).
[60] P. A. Conlon *et al.*, Solar Phys. **248**, 297 (2008).
[61] J. E. Pinzon, C. E. Puente, M. B. Parlange, and W. Eichinger, Boundary Layer Meteorol. **76**, 323 (1995).
[62] D. Schertzer and S. Lovejoy, in *Fractals: Physical Origin and Consequences*, edited by L. Pietronero (Springer, New York, 1989).
[63] J. G. V. Miranda, E. Montero, M. C. Alves, A. Paz Gonzalez, and E. Vidal Vazquez, Geoderma **134**, 373 (2006).
[64] E. M. de la Calleja Mora, J. L. Carrilo, M. E. Mendoza, and F. Donado, Eur. Phys. J. B **86**, 126 (2013).
[65] D. Benouioua, D. Candusso, F. Harel, and L. Oukhellou, Intl. J. Hydrogen Energy **39**, 21631 (2014).
[66] K. Matia, Y. Ashkenazy, and H. E. Stanley, Europhys. Lett. **61**, 422 (2003).
[67] V. S. L'vov, E. Podivilov, A. Pomyalov, I. Procaccia, and D. Vandembroucq, Phys. Rev. E **58**, 1811 (1998).
[68] W.-X. Zhou, D. Sornette, and W.-K. Yuan, Physica D **214**, 55 (2006).
[69] D. G. Stephen and J. A. Dixon, Chaos, Solitons Fractals **44**, 160 (2011).
[70] D. G. Stephen *et al.*, Chaos, Solitons Fractals **45**, 1201 (2012).
[71] D. G. Kelty-Stephen and J. A. Dixon, J. Exp. Psychol. **40**, 2289 (2014).
[72] S. Chang, M. C. Hsyu, H. Y. Cheng, and S. H. Hsieh, Chin. J. Physiol. **51**, 376 (2008).